Hydration, dehydration and dehydroxylation of bentonite from Lutila I deposit, Kremnické Vrchy Mts., Western Carpathians

Peter Uhlík[1*], Boris Guspan[1], Faisal A. Gread[1], Helena Pálková[2] & Marek Osacký[1]

[1] Department of Mineralogy, Petrology and Economic Geology, Faculty of Natural Sciences, Comenius University Bratislava, Mlynská dolina, Ilkovičova 6, 842 15 Bratislava, Slovakia; peter.uhlik@uniba.sk, guspanb@gmail.com, faisal.gread@yahoo.com, marek.osacky@uniba.sk
[2] Institute of Inorganic Chemistry, Slovak Academy of Sciences, Dúbravská cesta 9, Bratislava 845 36, Slovakia; helena.palkova@savba.sk
[*] Corresponding author

AGEOS

Abstract: Slovakia ranks among the five largest bentonite producers in Europe, with the Lutila I deposit in the Central Slovakia Volcanic Field representing one of its most significant bentonite resources. Despite its economic importance, information on the properties of this bentonite remains limited. Water loss through dehydration and dehydroxylation of two commercial bentonite samples from the Lutila I deposit was investigated at 105, 200, 400, 600, and 800 °C. The effects of temperature and interlayer cation composition on swelling behavior were also evaluated. These properties are important for applications related to supplementary cementitious materials (SCMs) and deep geological disposal of radioactive waste.

The RLU sample was a Na-activated bentonite containing 55 wt.% montmorillonite and 25 wt.% opal-C/CT, whereas the ELU sample was a natural Ca–Mg bentonite with 67 wt.% montmorillonite and 9 wt.% opal-C/CT. In both samples, dehydroxylation was characterized by a broad derivative thermogravimetry peak with a maximum near 665 °C, indicating cis-vacant montmorillonite. The ELU sample exhibited nearly twice the molecular water loss during drying (at 105 and 200 °C) compared with RLU, reflecting the presence of hydrated Ca^{2+} and Mg^{2+} interlayer cations associated with two water layers, whereas Na^{+} in RLU was associated with a single water layer.

RLU exhibited a substantially higher swell index than ELU. After heating to 400 °C, RLU retained approximately 35% of its original swelling capacity, whereas ELU lost its swelling capacity almost completely. Heating to 800 °C transformed montmorillonite in RLU predominantly into an amorphous phase, potentially enhancing pozzolanic reactivity. In contrast, ELU formed both an amorphous phase and a new crystalline phase, which may reduce the pozzolanic activity of the calcined material. The relative contributions of montmorillonite and opal-C/CT to total water loss were quantified for both samples. The results highlighted the critical role of interlayer cation composition in controlling the thermal behavior, swelling properties, and application potential of bentonites from the Lutila I deposit.

Key words: Lutila I bentonite deposit, calcium-magnesium and sodium montmorillonite, hydration, swelling, dehydration, dehydroxylation

1. INTRODUCTION

Bentonite is unique industrial raw material. The worldwide bentonite production is increasing mainly due to broad range of possible bentonite applications. Bentonite has high sorption and swelling capacity, plasticity, high specific surface area and high cation exchange capacity (CEC). These unique properties enable to use bentonites for many industrial applications such as: bonding clay in foundry, part of drilling fluid, ore pelletizing, pet litters, sorbent of various pollutants, engineering barrier for municipal and radioactive waste disposal, and recently also as supplementary cementitious material (SCM) and as organoclay for preparation of clay-polymer nanocomposites (e.g., Carrado & Komadel, 2009; Eisenhour & Brown, 2009; Christidis, 2011; Theng, 2012; Trümer et al., 2019; Coutelle et al., 2024a). Murray (2007) reported around other thirty examples of bentonite applications.

Bentonites consist predominantly of clay minerals from smectite group (most commonly montmorillonite). Due to the presence of smectites, bentonites have the above mentioned unique properties. Smectites have characteristic 2:1 type of layered structure consisting of one octahedral sheet interlayered between two tetrahedral sheets. The non-equivalent isomorphous substitution in the tetrahedral and octahedral sheets give rise to a charge imbalance which is compensated by exchangeable cations (e.g., Ca^{2+}, Mg^{2+}, Na^{+}, K^{+}) located in the interlayer space (e.g., Grim & Güven, 1978; Murray, 2007; Gilg et al., 2024). The octahedral sheet comprises three symmetrically independent positions that differ in the arrangement of hydroxyl groups and oxygen anions coordinating the central cation. In the trans-octahedral configuration, the hydroxyl groups occupy opposite vertices, whereas in the cis-octahedral configuration, the hydroxyl groups are situated along a common edge. In dioctahedral 2:1 layers, either the trans-octahedral site or one of the two symmetrically independent cis-octahedral sites may remain vacant, resulting in the formation of trans-vacant (tv) or cis-vacant (cv) layers (Tsipursky & Drits, 1984). Furthermore, the type, distribution of octahedral cations, and their distribution in the trans- and cis-positions significantly influence the chemical and thermal stability of the structure (Drits et al., 1995; Steudel et al., 2009).

Manuscript received 2026-06 04
Revised version accepted 2026-06-18

One of the most common features of smectites is the ability to expand and collapse the interlayer space. Loss of molecular water adsorbed on or within smectite particles can happen upon drying (dehydration; Derkowski et al., 2012). In the last fifteen years, new results on weakly and tightly bound molecular water in smectites and smectites behaviour during dehydration, dehydroxylation, and rehydration have been reported (e.g., Derkowski et al., 2012; Salles et al., 2010, 2015; Ferrage, 2016; Kuligiewicz & Derkowski, 2017; Emmerich et al., 2018; Derkowski & Kuligiewicz, 2022; Rybka et al., 2025). These results indicate that: 1.) weak-bonded water occurs on the surface of smectites and between the hydrated interlayer cations while the strong-bonded water hydrates these cations; 2.) smectites behaviour during dehydration and rehydration is affected by the interlayer cations and charge; 3.) the additional energy during rehydration may cause reexpansion of the collapsed interlayer space. Hydration and crystalline swelling involve the arrangement of water molecules into distinct interlayer planes, resulting in the formation of so-called mono-hydrated (1W), bi-hydrated (2W), and tri-hydrated (3W) states. Accordingly, the dehydrated state is referred to as the 0W state (Ferrage, 2016; Emmerich et al., 2018). The swelling behavior of smectite clay minerals is known to occur in two distinct regimes. Crystalline swelling involves the incorporation of a limited number of water layers into the interlayer space (up to 4W), whereas osmotic swelling corresponds to the complete delamination of clay layers in a solvent (Hotton et al., 2025). In essence, hydration is the driving process, involving the adsorption of water molecules onto interlayer cations and clay surfaces, whereas swelling represents the resulting physical expansion of the clay structure.

The dehydroxylation temperature of smectites represents a key parameter governing their thermal stability. Dehydroxylation occurs between 300 and 900 °C, as the release of a H_2O molecule formed by two adjacent OH groups from the octahedral sheet, leaving one residual oxygen atom in the structure. In the calcination of bentonites intended for use as partial replacements for Portland cement, the formation of a disordered, X-ray amorphous phase is considered advantageous, while achieving this transformation at the lowest possible temperature is desirable due to reduced energy consumption. Furthermore, the dehydroxylation temperature serves as an important criterion for the classification of smectites. Cis-vacant (cv) smectites exhibit dehydroxylation temperatures above 600 °C, whereas trans-vacant (tv) smectites dehydroxylate below 600 °C (Drits et al., 1995; Wolters & Emmerich, 2007; Emmerich et al., 2009; Derkowski & Kuligiewicz, 2022). In general, most smectites undergo dehydroxylation within the temperature range of 650–700 °C (Emmerich et al., 2009).

Most natural bentonite deposits consist of Ca-rich smectites rather than Na-rich (e.g., bentonite deposits in Montana and Wyoming). Ca-rich smectites are often treated by soda ash activation, in order to replace Ca with Na cation in the smectites interlayers (Bahranowski et al., 2021; Coutelle et al., 2024b). Both Na-bentonites (dominated by Na-rich smectites) and Ca-bentonites (dominated by Ca-rich smectites) are important technological types of bentonites having distinct properties and therefore different applications. Generally, Ca-bentonites have excellent sorption properties, whereas Na-bentonites have significantly greater swelling ability compared to Ca-bentonites (Murray, 2007; Coutelle et al., 2024b).

Bentonite represents one of the most important industrial minerals in the Slovak Republic. The first Slovak bentonite deposits were explored in the 1950s within the East Slovak Neogene Basin (Gregor & Číčel, 1969). The most significant and highest-quality bentonite deposits in Slovakia are situated in the Central Slovakia Volcanic Field, particularly within the Jastrabá Formation in the Kremnické vrchy Mts., which is predominantly composed of various rhyolitic rock types (Lexa et al., 1998; Zuberec et al., 2005; Baláž et al., 2015; Osacký et al., 2019; Uhlík et al., 2024). These bentonites contain approximately 70–80 wt.% of montmorillonite.

Over the past two decades, bentonite exploration in Slovakia has intensified considerably, resulting in the discovery and exploitation of several new deposits alongside previously known occurrences. During the 21st century, bentonite production in Slovakia has increased nearly fivefold. In 2024, total bentonite production reached 309 kt (Šoltés et al., 2024), placing Slovakia among the leading bentonite-producing countries worldwide. Simultaneously, the Slovak Republic ranks among the top five European producers of bentonite (Hlavný banský úrad, 2025; Simmons, 2025).

Research on Slovak bentonites has a long-standing tradition (e.g., Gregor and Číčel, 1969; Slávik et al., 1971; Kraus et al., 1982, 1989, 1994; Madejová et al., 1995, 2017; Janotka et al., 2002; Honty et al., 2004; Šucha et al., 2005; Andrejkovičová et al., 2008; Galamboš et al., 2009; Uhlík et al., 2012; Komadel & Madejová, 2013; Adamcová et al., 2014; Bizovská et al., 2016; Pentrák et al., 2018; Osacký et al., 2019; Slaný et al., 2023; Gread et al., 2025, 2026), and the resulting scientific contributions have gained international recognition.

The Lutila I bentonite deposit is a relatively recently opened deposit located in the southwestern part of the Kremnické vrchy Mountains, approximately 7 km south-southeast of the town of Kremnica. The deposit has been exploited by REGOS, s.r.o. since 2013. The updated reserves of the deposit in 2019 were 2 Mt. In 2024, annual bentonite production from the Lutila I deposit reached 58.6 kt, ranking it among the three most productive bentonite deposits in Slovakia, together with Kopernica III (63.6 kt; operator: BENOX s.r.o.) and Stará Kremnička – Jelšový potok (60 kt; operator: Kremnická banská spoločnosť, s.r.o.) (Hlavný banský úrad, 2025). Bentonite from the Lutila I deposit is currently utilized primarily as technical bentonite in foundry applications, the construction industry, environmental sealing barriers, and as lumpy cat litter. The deposit originated through the bentonitization of the marginal glassy/perlitic carapace of extrusive domes (Uhlík et al., 2024).

Systematic investigation of the Lutila I bentonite deposit, focusing on its mineralogical and chemical composition, physicochemical properties, genesis, and potential industrial applications, has only been initiated since 2020. The present study represents one of the first outputs of this research effort and focuses on key bentonite properties, namely hydration, swelling, dehydration, and dehydroxylation. These properties are critical for a wide range of industrial applications, including

engineered barriers for waste disposal (particularly radioactive waste), supplementary cementitious materials (SCMs), cosmetics, and desiccants (Murray, 2007). However, despite their importance, these characteristics of Slovak bentonites remain insufficiently studied.

The main objective of this work is to evaluate the behavior and stability of Na-activated and non-activated bentonites under varying temperature conditions, with particular emphasis on the influence of temperature and interlayer cation composition on swelling behavior. The swelling index was determined under ambient conditions and after thermal treatment up to 400 °C, in order to improve understanding of the thermal stability of bentonite, which is crucial for its use in deep geological disposal systems for radioactive waste. In addition, dehydroxylation processes were investigated as a key parameter for assessing the suitability of bentonite as a supplementary cementitious material (mainly temperatures at 600 and 800 °C).

2. MATERIALS AND METHODS

The investigated initial material consisted of two commercial bentonite samples from the Lutila I deposit in the Kremnické vrchy Mountains. The RLU sample represented a Na-activated bentonite supplied by Romin Slovakia, spol. s r. o., whereas the ELU sample corresponded to a natural Ca–Mg bentonite provided by Envigeo, a.s. Both samples were processed by grinding and drying to a particle size fraction <63 μm and were used as initial samples for further treatments and tests.

2.1 Thermal analyses (TA) and thermal treatment of initial bentonites

Loss on drying (LOD) is a widely applied analytical method used to determine the moisture content (H_2O) of a sample at 105 °C. Approximately 2 g of each sample was accurately weighed, and the exact mass was recorded before drying at 105 °C for 18 h in a laboratory oven (Memmert UNE 600) at Comenius University Bratislava. After drying, the samples were weighed, and LOD was calculated. Subsequently, dried samples were transferred to a muffle furnace (MLW LM 212.11) at Comenius University Bratislava, where calcination was performed at 400 °C, 600 °C, and 800 °C (± 10 °C) for 4 h. Following calcination, the samples were reweighed, and the loss on ignition (LOI) values were determined. For the LOD measurements, up to 12 parallel samples were analyzed, whereas four parallel samples were used for the LOI determinations.

Two moisture analyzers (OHAUS MB45) were employed for the initial samples (ELU and RLU) at Comenius University Bratislava. The instruments were operated simultaneously under identical experimental conditions to perform parallel measurements. The analyzers were programmed to specific temperatures of 105 °C and 200 °C using the "standard" heating mode. The percentage of mass loss, corresponding to the moisture content, was automatically calculated by the instrument software. The effect of the weight was also partially tested, and weights of 3, 5, 7, and 10 g were used.

Samples after heat treatment were labeled with the original name, to which was added a number indicating the drying or calcination temperature (e.g., RLU 200 or ELU 600).

Thermogravimetric (TG), derivative thermogravimetric (DTG), and differential thermal analysis (DTA) of the initial samples RLU and ELU were performed using a NETZSCH STA 449 F3 Jupiter analyzer at Institute of Inorganic Chemistry, Slovak Academy of Sciences in the temperature range 20–1000 °C by analyzing 40 mg of sample in a 10 K/min heating rate and a N_2 flow rate of 50 ml/min. The samples were stored at ambient laboratory conditions and measured without any pretreatment.

2.2 X-ray diffraction (XRD)

Quantitative X-ray diffraction (QXRD) was performed on randomly oriented preparations of initial and thermally treated samples. The mineral quantities were retrieved using RockJock software (Eberl, 2003). Samples were prepared according to the method modified by Omotoso and Eberl (2009) and reported by Środoń et al. (2001). The sample was passed through a 250 μm sieve, then 1 g of sample was mixed with 0.250 g of corundum (internal standard) and micronized with 4 ml of denatured ethanol (96%) in a McCrone Micronizing Mill with yttrium-stabilized zirconium oxide grinding cylinders for 5 min. Then the mixture was dried overnight at 60 °C. The mixture (sample + corundum) was then shaken for 10 min in a plastic vial (25 ml) with 3 plastic balls (9 mm diameter) using a Retsch MM 200 mill, n-Hexane was added to the mixture (to minimize the preferred orientation) in the ratio of maximum 0.5 ml hexane to 1 g of pure clay, and the vial was shaken for an additional 10 min. The powder was then top loaded into an XRD holder after passing through 250 μm sieve and X-rayed from 2° to 65° with a step size of 0.02°2θ and a counting time of 2 s per step using BRUKER D8 ADVANCE diffractometer at Comenius University Bratislava equipped with CuKα radiation (λ_{a1} = 1.54060 10^{-10} cm) and a graphite monochromator, operated at beam current 40 mA, and accelerating voltage 40 kV.

2.3 Swell index determination

The swell index of bentonite was determined in accordance with the standard test method ASTM D5890 (2011) at Comenius University Bratislava. The measurements were performed on bentonite samples (ELU and RLU) prior to thermal treatment (25 °C) and after heating at 105 °C, 200 °C, 400 °C, and 800 °C.

Initially, the volume of approximately 2 g of each dry sample was measured and recorded as 2 ml. Subsequently, 100 ml graduated measuring cylinders were filled with 100 ml of distilled water. Two g of each sample was weighed onto Petri dishes. The prepared samples and measuring cylinders were arranged side by side, and the samples were gradually and uniformly added to the water surface using spatulas to ensure even distribution. This procedure was repeated until the entire sample mass had been transferred into the measuring cylinders. Swelling samples began adsorbing moisture immediately upon contact with water, forming floating agglomerates at the surface before gradually settling to the bottom of the cylinder. In contrast, non-swelling samples

became wetted rapidly and sedimented almost immediately. The test results were expressed as the swell index (final swollen volume), which was read directly from the graduated scale of the measuring cylinders (Fig. 1). The swell index expressed as ml/2 g to the nearest 0.5 ml after a minimum 16 h hydration period from the last bentonite powder increment addition has been recorded. Mean values were subsequently calculated from two parallel measurements for each sample. The swelling factor was determined as the ratio between the swell index in water and the initial dry sample volume measured prior to immersion.

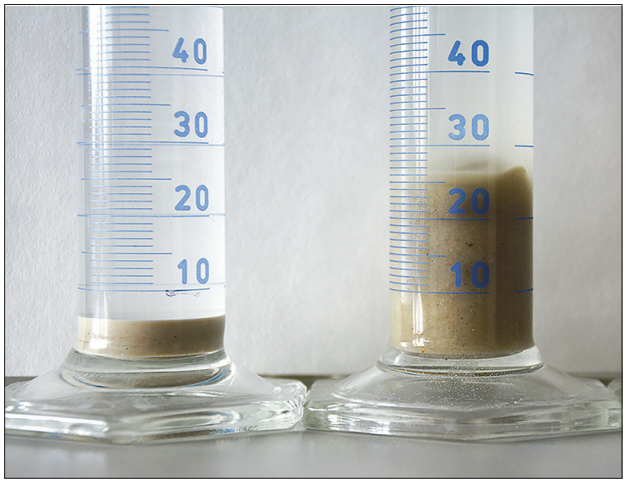

Fig. 1. Example of swelling bentonites after Swell index test (ASTM D5890). ELU at 25 °C left and RLU at 25 °C right.

2.4 Chemical analysis

Both initial samples were analyzed at Bureau Veritas Commodities Canadas Ltd. (Vancouver, Canada). Inductively Coupled Plasma Emission Spectroscopy (ICP–ES) was used. The detection limits ranged from 0.002–0.04 wt.%.

3. RESULTS AND DISCUSSION

3.1 Characterization of the initial material

The dominant mineral phase identified in both studied samples was montmorillonite, belonging to the smectite group. This was confirmed by the presence of characteristic X-ray diffraction (XRD) diffraction peaks, particularly the 060 peak with a maximum at 61.85° 2θ (Fig. 2). The corresponding d-spacing value of 1.50 Å is characteristic of dioctahedral smectite, specifically montmorillonite (Moore & Reynolds, 1997). The ELU sample contains 67 wt.% montmorillonite and RLU 55.5 wt.% (Table 1).

The position of the basal 001 diffraction peak further indicates differences in the interlayer cation composition of the investigated samples. The natural, untreated bentonite sample (ELU) exhibits a basal spacing of 15.24 Å (5.84° 2θ, Fig. 2a), which is indicative of the presence of divalent interlayer cations, predominantly Ca^{2+} and Mg^{2+}, within the montmorillonite structure. The occurrence of these cations is typical for bentonites originating from the Kremnické vrchy region (e.g., Čičel et al., 1992; Šucha et al., 2005; Górniak et al., 2016; Osacký et al., 2019).

In contrast, the Na-activated sample (RLU) displays a basal spacing of 12.5 Å (7.08° 2θ, Fig. 2b), confirming the predominance of monovalent Na^+ ions in the interlayer space. The higher Na content in the RLU sample was also confirmed by chemical analysis (Table 2). The observed difference in d-spacing between the two samples was associated with the substantially higher hydration enthalpy of divalent cations (Mg^{2+} = 1921 kJ·mol^{-1}; Ca^{2+} = 1577 kJ·mol^{-1}) compared to monovalent Na^+ ions (409 kJ·mol^{-1}). Consequently, divalent cations promote the formation of two layers of interlayer water molecules, whereas monovalent sodium typically stabilizes only a single water layer (Smith, 1977; Salles et al., 2015; Ferrage, 2016; Derkowski & Kuligiewicz, 2022).

In addition to hydrated clay minerals, other thermally unstable phases may significantly affect the resulting mass loss values during thermal analysis (TA), including carbonates, sulphates, and organic matter (e.g., Emmerich, 2010; Derkowski & Kuligiewicz, 2022). However, these impurities were not detected in the studied bentonite samples (except for a negligible amount of calcite in the sample RLU, which was probably a relic of soda ash activation – Table 1); therefore, the observed mass loss can be interpreted directly as water loss. Among the hydrated phases present, only opal-C/CT may substantially influence the measured water loss values in the investigated samples. This aspect is discussed in a later section.

Thermogravimetric analysis (TGA) confirmed the presence of different interlayer cations in the investigated samples. Monovalent interlayer cations are typically associated with a single dehydration peak on DTG curves at approximately 100 °C, whereas divalent cations produce either two distinct DTG dehydration peaks or a pronounced high-temperature shoulder extending up to ~200 °C (Fig. 3; Derkowski & Kuligiewicz, 2022).

TGA additionally enabled the determination of mass loss associated predominantly with the dehydroxylation of smectite, corresponding to the release of structural OH groups. In both samples, dehydroxylation was represented by a broad DTG peak with a maximum at approximately 665 °C (Fig. 3), indicating the predominance of cis-vacant dioctahedral smectites (Drits et al., 1995; Wolters and Emmerich, 2007). The occurrence of cis-vacant montmorillonite has also been reported by Osacký et al. (2019) in bentonite samples from three deposits located in the Kremnické vrchy Mountains, namely Lutila I, Stará Kremnička – Jelšový potok, and Stará Kremnička III.

K-feldspar and opal-C/CT represent additional mineral phases with relatively high abundances in both investigated samples. Opal-C and opal-CT cannot be clearly distinguished based on XRD (Jones, 2021), therefore, we do not exclude the presence of both and refer to the determined opaline silica as Opal-C/CT. A pronounced difference was observed in the content of opal-C/CT, which reaches 25 wt.% in the RLU sample, compared to only 9 wt.% in the ELU sample (Fig. 2, Table 1, 2). Other identified mineral phases include plagioclase, quartz, and biotite, each occurring at concentrations below 5 wt.%, while goethite, ilmenite, rutile, and apatite were present only in trace amounts (<0.5 wt.%; Table 1).

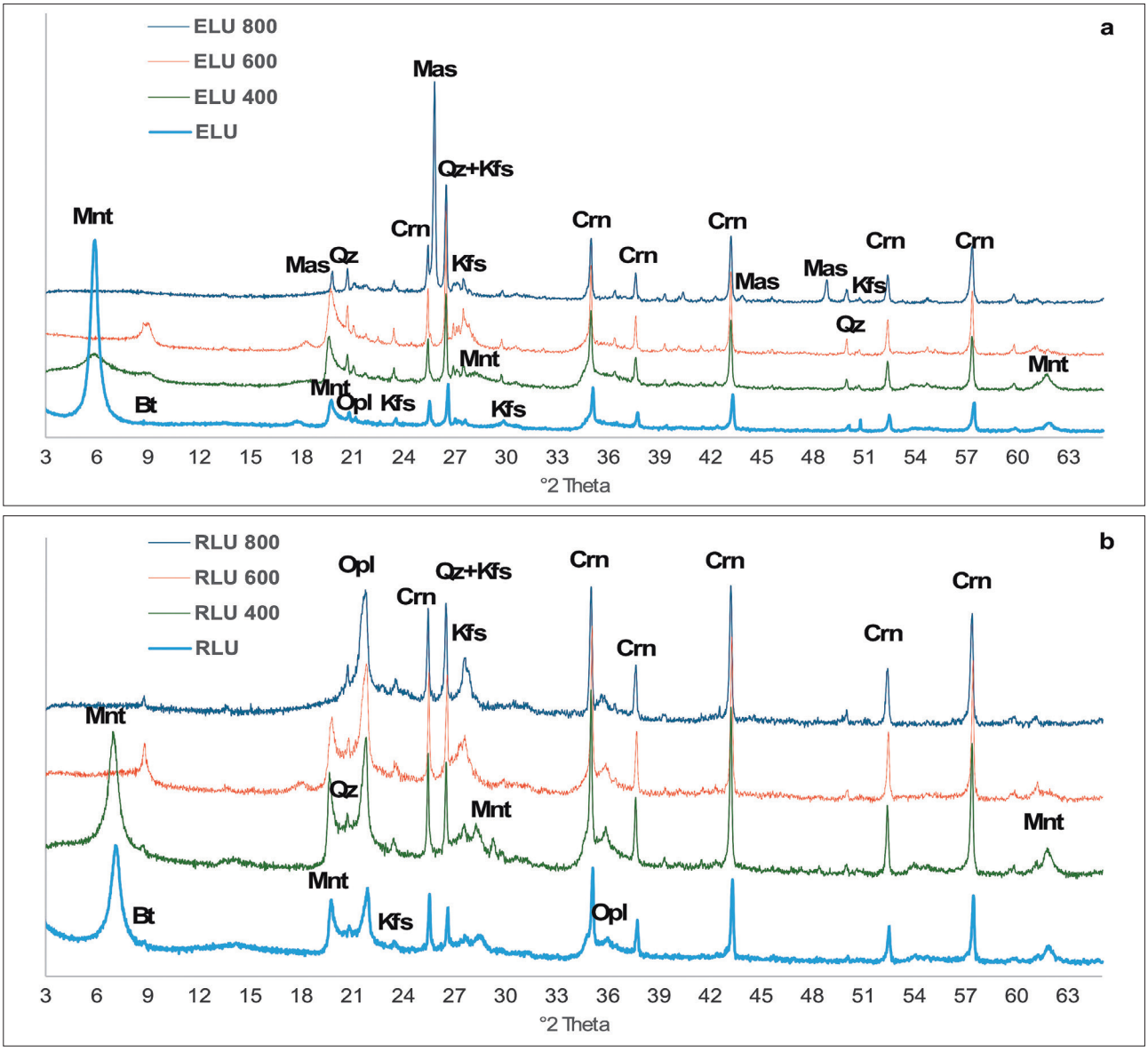

Fig. 2. XRD patterns of randomly oriented samples before and after heating. a. ELU, b. RLU. Mnt= montmorillonite; Qz = quartz; Bt = biotite; Kfs = K-feldspars; Opl = opal-C/CT; Mas = magnesium aluminum silicate phase; Crn = internal standard (corundum),

The differing proportions of montmorillonite and opal-C/CT suggest partial mineralogical heterogeneity within the Lutila I deposit. Both phases originate from the alteration of volcanic glass, opal-C/CT precipitates from residual dissolved silica released during the transformation of volcanic glass into montmorillonite (Grim, 1962). Elevated opal-C/CT contents could indicate limited fluid migration during alteration processes, which was insufficient to effectively remove residual SiO_2 from the system (Christidis and Huff, 2009; Gread et al., 2026).

3.2 Dehydration of Lutila I bentonite

After 18 h of drying at 105 °C in a laboratory drying oven, the loss on drying (LOD) of the RLU sample reached 6.99 wt.% of the original mass, whereas the ELU sample exhibited an almost twofold higher LOD of 12.28 wt.% (Fig. 4). These LOD values represent weakly bound water (Kuligiewicz & Derkowski, 2017).

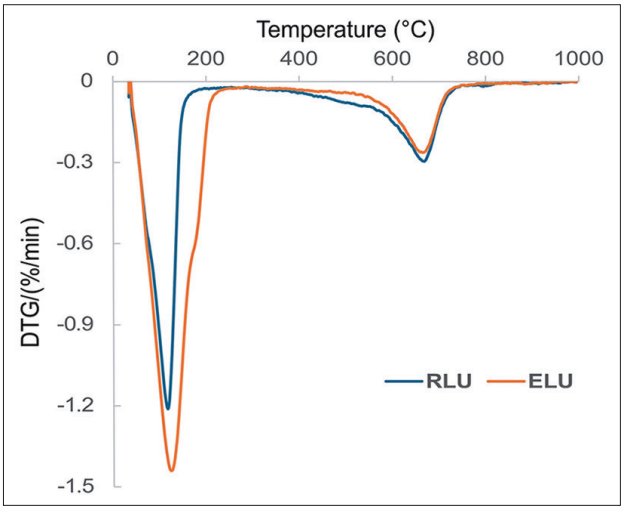

Fig. 3. DTG curves of initial bentonites.

Tab. 1. The mineralogical composition (wt.%) of the analyzed bentonites by XRD, before and after heating, determined using RockJock.

	RLU	RLU 400	RLU 600	RLU 800	ELU	ELU 400	ELU 600	ELU 800
Quartz	1-May	2	3	3	5-Feb	5-May	8-Aug	9
K-feldspars	12-May	12-May	11	7-May	14	11-Apr	15-Jul	10
Plagioclase	1	2-Jan	5-May	4-May	1	2-May	7-May	0.5
Goethite	<0.5				0.5			
Rutile + ilmenite	<0.5	<0.5	<0.5		<0.5	<0.5	<0.5	<0.5
Opal-C/CT	25	25-Jan	30	19	9	9-Feb	10	6-May
Montmorillonite	55.5	52.3	34.3	3?	67	68	55	5?
Biotite	3	2-Sep	1-Jul	1-May	2-Mar	2-Apr	2	1
Apatite	<0.5	<0.5	<0.5	<0.5	<0.5	<0.5	<0.5	<0.5
Calcite	<0.5	2-Jan						
New phase								20
Amorphous phase			13-May	61				47
Full pattern degree of fit	0.0751	0.0611	0.0518	0.0531	0.0869	0.0601	0.0850	0.112

Tab. 2. Chemical compositions (%) of initial bentonites.

	RLU	ELU
SiO_2	61.13	57.48
Al_2O_3	15.88	16.20
Fe_2O_3	2.05	2.05
MgO	2.01	3.16
CaO	1.44	1.72
Na_2O	3.23	0.45
K_2O	1.43	1.00
TiO_2	0.14	0.08
P_2O_5	0.02	<0.01
MnO	0.03	0.06
Cr_2O_3	<0.002	<0.002
LOI	12.4	17.6

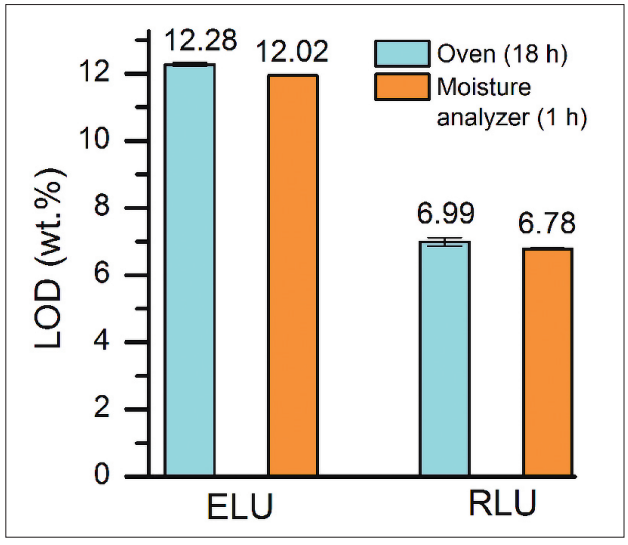

Fig. 4. LOD at 105 °C determined using overnight oven drying (18 h) and a moisture analyzer (1 h); standard deviations are shown.

The significantly higher LOD observed for the ELU bentonite sample can be only partly attributed to the higher content of montmorillonite (Table 1, difference was only 11.5 wt.%). The difference was mostly caused by the presence of hydrated divalent calcium and magnesium cations associated with two layers of interlayer water, in contrast to the RLU bentonite sample containing hydrated monovalent sodium cations with only a single layer of water molecules (e.g., Christidis, 2013; Emmerich, 2013; Derkowski & Kuligiewicz, 2022).

Using a moisture analyzer with continuous monitoring, the most pronounced mass loss at 105°C, corresponding to the weakly bound water, occurred during the first 10 min of drying, after which the decrease in sample mass became considerably slower. For example, in the ELU sample with a 5 g initial mass, the mass loss between 15 and 60 min amounted to only 0.5 wt.%. In the ELU sample with a higher initial mass (10 g), the stabilization of LOD values required a longer time, approximately 30 min, compared to the lower sample mass (Fig. 5a). This confirms that the rate of water release is also influenced by the sample

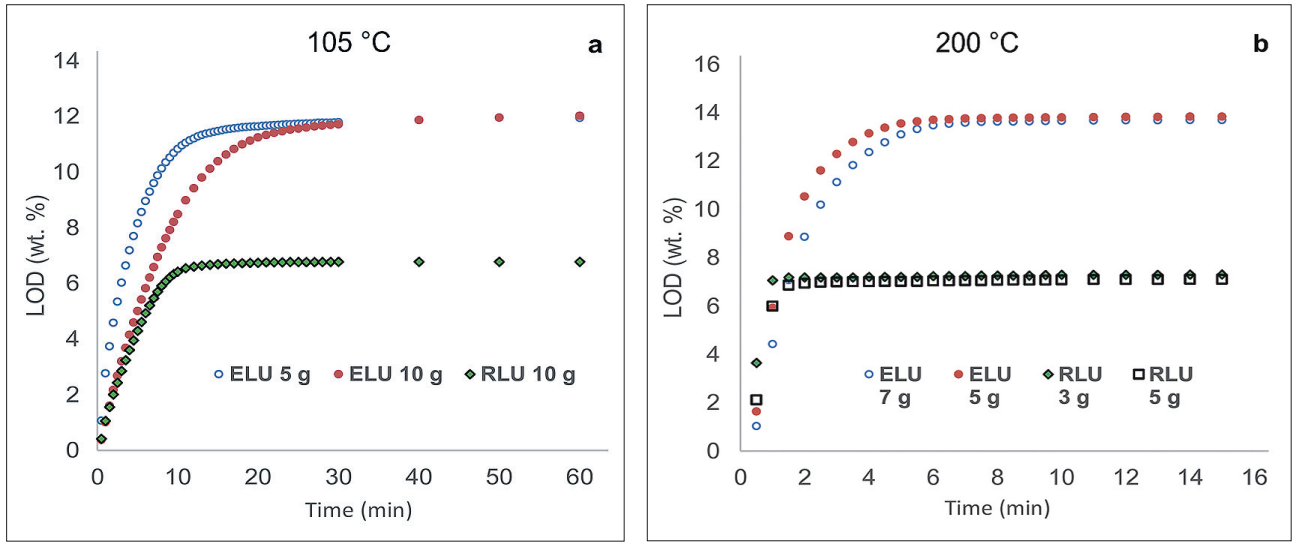

Fig. 5. LOD curves of initial bentonites with different analysed weight determined using moisture analyzer in time range 0–60 min. at 105 °C (a.) and in time range 0–15 min. at 200 °C (b).

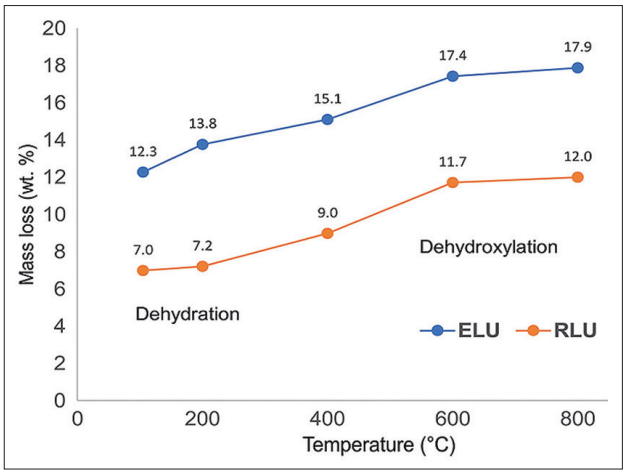

Fig. 6. Mass loss of the studied bentonites after drying in a laboratory oven (105 and 200 °C) and heating in a muffle furnace (400, 600, and 800 °C).

mass and highlights the importance of following a standardized procedure, including consistent sample weighing.

The LOD values determined at 200 °C were higher than those obtained at 105 °C, relatively by 6% for the RLU sample (7.21 wt.%) and by 15% for the ELU sample (13.77 wt.%; Fig. 5, 6). These results indicate the presence of residual, tightly bound water in smectite (e.g., Środoń & McCarty, 2008; Kuligiewicz & Derkowski, 2017; Rybka et al., 2025). The gradual release of tightly bound montmorillonite interlayer water occurred up to approximately 250 °C, according to DTG curves (Fig. 3). At 200 °C, the majority of molecular water in the RLU sample was released within less than 2 min, irrespective of sample mass. In contrast, the ELU sample, characterized by a higher water content, required up to 6 min for the release of most molecular water, also independently of sample mass, and the process occurred more gradually (Fig. 5b). These observations confirmed that divalent cations bind water molecules more strongly than monovalent cations (Webb et al., 1986; Derkowski & Kuligiewicz, 2022). The Mg^{2+} cation can hold H_2O molecules even beyond 550 °C (Kuligiewicz & Derkowski, 2017).

The moisture analyzer enabled substantially faster determination of LOD compared to the standard oven-drying method, which typically requires 12 h or drying until no further mass loss is observed (Lang et al., 2017). Nevertheless, slight differences were identified between the LOD values obtained using the two methods, which are related primarily to the drying duration (e.g., Varga et al., 2019; Rybka et al., 2025). For the ELU sample, the relative difference between 1 h and 18 h drying at 105 °C was 2.8% (absolute difference of 0.34 wt.%), whereas for the RLU sample, the relative difference was 3.0% (absolute difference of 0.21 wt.%). These differences were approximately three times greater than the standard deviation associated with LOD measurements obtained using the drying oven method.

3.3 Dehydroxylation of Lutila I bentonite

The dehydroxylation of both studied Lutila I bentonites was investigated using TGA (Fig. 3), XRD (Fig. 2, Table 1), and LOI (Fig. 6). The XRD patterns of the initial samples and those heated to 400 °C were nearly identical, indicating the absence of significant structural changes in the identified mineral phases. The only notable difference was a substantial decrease in the intensity of the first basal reflection (00l; 15.24 Å), accompanied by the appearance of a broader and more intense peak at 10 Å in the ELU sample. This observation may indicate the onset of smectite interlayer collapse, potentially caused by the migration of Mg^{2+} into octahedral vacancies (Kaufhold et al., 2016). The fixation of Mg^{2+} is also expected because Mg^{2+} represents the smallest interlayer cation among those present in the studied samples (Shannon, 1976; Rybka et al., 2025).

The disappearance of the 00l diffraction peak and the appearance of the 10 Å reflection were observed in both samples after heating to 600 °C. These changes indicated a complete collapse of the smectite interlayer space and its transformation into a mica-like interlayer structure. Although a decrease in the intensity of the montmorillonite 060 reflection (1.50 Å) suggested partial structural disruption, the hkl reflection at 19.6 °2θ (4.48 Å) remained unchanged (Fig. 2). Quantitative X-ray diffraction (QXRD) analysis revealed that the montmorillonite content decreased in both samples after heat treatment from 400 to 600 °C, by 18 wt.% in RLU and 13 wt.% in ELU (Table 1). In the RLU sample, this decrease was compensated by the identification of an amorphous phase using QXRD, together with an increase in the amount of opal-C/CT, which may also be associated with the development of amorphous material. In the ELU sample, the reduction in montmorillonite content was accompanied by an apparent increase in quartz and feldspar contents (Table 1); however, this increase was considered to be relative rather than absolute.

Following heating to 800 °C, all montmorillonite reflections disappeared from the diffraction patterns of both bentonite samples (Fig. 2), although QXRD still detected minor amounts of montmorillonite (Table 1). A substantial proportion of the amorphous phase was identified by QXRD using a volcanic glass standard. In addition, several new intense diffraction peaks appeared in the XRD pattern of the ELU sample (Fig. 2a). Their d-spacing values (4.47, 3.44, 2.23, 1.86, and 1.61 Å) correspond closely to the magnesium aluminum silicate phase $MgAl_2Si_4O_{12}$ with a high-quartz structure. This phase was previously synthesized by Schulz et al. (1971) from glass of identical composition at 977 °C within one hour.

To the best of our knowledge, the formation of this phase during the thermal treatment of bentonite or smectite has not been reported in the literature. Furthermore, the relatively low temperature at which this phase formed is noteworthy. Previous studies reported the formation of new phases such as β-quartz, cristobalite, cordierite, anorthite, or mullite only at temperatures of 1000 °C or higher (e.g., Grim & Kulbicki, 1961; Fajnor and Kuchta, 1985; Garg and Skibsted, 2014). The presence of this phase, therefore, should be verified by additional thermal experiments on new samples and complementary analytical techniques in future work.

The mass loss observed in both studied bentonites cannot be attributed exclusively to the dehydration and dehydroxylation of montmorillonite (Fig. 6). Both samples contain opal-C/CT, with the RLU sample comprising up to 25 wt.% of this phase.

Opaline SiO_2 contains water in several forms, including silanol groups (OH groups bonded to silicon) and two types of molecular water: isolated water molecules trapped within silica beads and hydrogen-bonded water molecules located in pores between the silica beads (Flörke et al., 1991; Jones, 2021). The total water content of opaline silica is highly different, ranging from approximately 1 to 14 wt.%, and its release depending on temperature is also very variable. Previous studies have shown that the majority of water loss from opaline silica occurs over a broad temperature range extending to approximately 1000 °C. (e.g., Flörke et al., 1991; Graetsch, 1994; Thomas et al., 2020; Jones, 2021). In general, the dehydroxylation of smectites occurs within a broad temperature interval of approximately 300–900 °C (Derkowski & Kuligiewicz, 2022), indicating that the release of water from montmorillonite and opal-C/CT occur simultaneously. Nevertheless, the application of multiple analytical approaches enables at least a partial distinction between these overlapping processes. The contribution of water released from opaline silica can be identified from the TGA data (Fig. 3). When the broad dehydroxylation interval characteristic of smectites is constrained to the principal dehydroxylation range of low- to medium-charge montmorillonites, corresponding to the montmorillonites from the Kremnické vrchy Mts., the relevant temperature interval is narrowed to approximately 500–750 °C (Wolters and Emmerich, 2007; Emmerich et al., 2009; Osacký et al., 2019; Derkowski & Kuligiewicz, 2022).

Following the initial stage of intensive dehydration, the mass loss of both bentonite samples began again to increase gradually from approximately 300 °C onward. From this temperature, the DTG curves progressively diverged, reaching the greatest difference at approximately 520 °C, where the RLU sample exhibited a higher mass loss despite its lower montmorillonite content and higher opal-C/CT abundance (Fig. 3; Table 1). Consistently higher mass losses were also recorded for the RLU sample within the LOI and TGA temperature intervals between 200 and 600 °C (Table 3). These observations indicated that a substantial proportion of the mass loss occurring between 200 and 800 °C could also be attributed to water release from opal-C/CT in both studied samples. A simple calculation was performed to obtain a qualified estimate of the water loss associated with montmorillonite and opal-C/CT in both investigated bentonite samples (Table 4). The calculation was based on the mass loss recorded between 200 and 800 °C by TGA (Table 3), the phase abundances determined by QXRD (Table 1), and the reported dehydroxylation mass loss of pure montmorillonite, ranging from 4.7 to 4.9 wt.% (Derkowski & Kuligiewicz, 2022). Using these parameters, the contribution of montmorillonite to the total weight loss was first calculated to be 2.64 wt.% for the RLU sample and 3.22 wt.% for the ELU sample (Table 4). The remaining mass loss was subsequently attributed to opal-C/CT, enabling the calculation of the water content of the pure opaline SiO_2 phase based on its QXRD-derived abundance. The resulting water contents were estimated at 12.48 wt.% for opal-C/CT in sample RLU and 7.16 wt.% in sample ELU (Table 4). Although these values differ substantially, they remain within the broad range of water contents reported for opaline silica phases in the literature (Flörke et al., 1991; Jones, 2021).

Dehydroxylation of clay minerals is an important reaction when assessing their potential for use as SCM (e.g., Ayati et al., 2022; Snellings et al., 2023). Alumina and silica are the principal constituents of most naturally occurring clay minerals, making them potential SCMs for partial cement replacement. In their natural state, however, clay minerals possess a stable crystal lattice in which alumina and silica exhibit limited reactivity. Heat treatment can disrupt this structure, increasing disorder, preferably in the form of aluminosilicate glass, and increasing pozzolanic reactivity. The pozzolanic reaction occurs under alkaline conditions in cementitious systems and involves the consumption of calcium hydroxide generated during the hydration of Portland cement (Garg and Skibsted, 2014; Trümer et al., 2019; Snellings et al., 2023).

Clay raw materials rich in illite, mixed-layer illite–smectite (I–S), or smectite generally develop significant pozzolanic reactivity after calcination at temperatures exceeding 800 °C (Garg and Skibsted, 2014; Trümer et al., 2019; Ayati et al., 2022). Compared with activated illitic and kaolinitic clays, calcined bentonite exhibits intermediate pozzolanic performance (Fernandez et al., 2011; Schulze & Rickert, 2019). As bentonite is predominantly composed of montmorillonite, its pozzolanic activity after calcination can be attributed to the combined effects of a high content of amorphous phases, formed as metastable products of montmorillonite decomposition, and a relatively high specific

Tab. 3. Mass loss of the studied bentonites in different temperature ranges determined by LOI and TGA methods. Values are given in wt.%.

	LOI		TGA	
	ELU	**RLU**	**ELU**	**RLU**
25–200 °C	13.8	7.2	12.5	7.1
25–800 °C	17.9	12.0	16.4	12.9
200–400 °C	1.3	1.8	0.6	0.7
200–600 °C	2.3	2.7	1.6	2.3
200–800 °C	4.1	4.8	3.9	5.8
400–600 °C	2.8	3.0	1.0	1.6
600–800 °C	0.5	0.3	2.2	3.4
800–1000 °C			0.1	0.3
25–1000 °C			16.5	13.2

Tab. 4. Calculation of water released (wt.%) from montmorillonite (Mnt) and opal-C/CT using the mass loss recorded between 200 and 800 °C by TGA (Table 3), the phase abundances determined by QXRD (Table 1), and * the published dehydroxylation mass loss of pure montmorillonite (Derkowski & Kuligiewicz, 2022). ** amount of Montmorillonite; *** amount of opal-C/CT determined by QXRD.

	Measured	Calculated		
	200-800 °C	**Mnt**	**Opal-C/CT**	
100 % mont	4.8*			
RLU (55.5 %)**	5.76	2.64	3.12	
ELU (67 %)**	3.86	3.22	0.64	
			1%	100%
RLU (25 %)***			0.12	12.48
ELU (9 %)***			0.07	7.16

surface area compared with conventional SCMs (Trümer et al., 2019). Nevertheless, determining the optimum calcination temperature required to maximize the pozzolanic reactivity of clay raw materials remains a significant challenge. Recent methodological advances have enabled a substantial reduction in the time required for the preliminary assessment of the pozzolanic activity of potential supplementary cementitious materials (SCMs), thereby facilitating the investigation of a broader range of materials with respect to their mineralogical composition, calcination temperature, and calcination duration (Avet et al., 2016; Snellings & Scrivener, 2016; Min et al., 2025). The results of the present study indicated that the nature of exchangeable cations represents an additional key parameter in evaluating the suitability of bentonites as SCM precursors. It was hypothesized that the presence of Mg in both exchangeable and octahedral positions, together with a favourable Al_2O_3–SiO_2–MgO compositional ratio related to mineralogical composition in the ELU bentonite sample, promoted the crystallization of a new phase at the relatively low temperature of 800 °C (Fig. 2B; Table 1). The formation of this crystalline phase is expected to adversely affect the pozzolanic reactivity of the thermally activated bentonite. In contrast, the predominance of Na among the exchangeable cations may contribute to a reduction in the melting temperature and facilitate the formation of an amorphous phase at lower calcination temperatures, thereby enhancing pozzolanic performance. The evaluation of pozzolanic activity across a wider spectrum of clay-rich raw materials, including both high- and low-grade bentonites from the Western Carpathians, will constitute an important direction of future research. Nevertheless, prior to the implementation of new raw materials as SCMs, comprehensive testing is required, including more time-intensive performance assessments such as concrete compressive strength testing (e.g., Badogiannis and Tsivilis, 2009; Janotka et al., 2010; Bačuvčík et al., 2022).

3.4 Influence of interlayer cations and thermal treatment on swelling of bentonite

The swell index and swelling factor measured at room temperature (25 °C) differed significantly between the studied bentonites (Table 5; Figure 7). Both parameters were 4.9 times higher for the RLU sample than for the ELU sample. This result was expected, as RLU represents a Na-activated bentonite, whereas ELU retains its original exchangeable cation composition.

Thermal treatment at 105 °C and 200 °C resulted in a slight increase in swelling capacity for both bentonites. However, XRD observations of sample ELU 400 (Fig. 2a), indicating the onset of smectite interlayer collapse, likely associated with the migration of Mg^{2+} ions into octahedral vacancies (Kaufhold et al., 2016; Rybka et al., 2025), were subsequently confirmed by the swell index test. After heating to 400 °C, sample ELU exhibited almost no measurable swelling. In contrast, sample RLU 400 retained approximately 35% of its original swelling capacity (Table 5, Fig. 7). These results highlight the influence of interlayer cation characteristics on the thermal stability of smectite. The larger ionic radius of Na^+ (116 pm) compared to Ca^{2+} and Mg^{2+} (114 pm and 86 pm, respectively; Shannon, 1976; Rybka et al., 2025) appears to contribute to the partial preservation of the swelling ability after thermal treatment. Rybka et al. (2025) documented rehydration capacities of 50%, 57%, and 27% for highly charged montmorillonite (SCa-3) in homoionic Na^+, Ca^{2+}, and Mg^{2+} forms, respectively, following dehydration at 300 °C. Our new data and their results indicated that substantial structural changes occurred between 300 and 400 °C, with only the Na-activated RLU sample maintaining a significant swelling capacity after heating to 400 °C. However, further investigation is required to evaluate other key barrier properties, including hydraulic conductivity, diffusion behavior, radionuclide retention, and long-term structural stability following heating at 400 °C.

The partial preservation of swelling in sample RLU 400 is particularly relevant for the disposal of radioactive waste, where bentonite should serve as a critical component of engineered barrier systems. Previous studies suggested that a maximum canister temperature below 100 °C is appropriate for repositories hosted in crystalline rocks, whereas higher temperatures, potentially approaching 300 °C, may be acceptable in alternative host-rock environments (Sellin & Leupin, 2013; Kuligiewicz & Derkowski, 2017; Kaufhold et al., 2023). The observed thermal stability of the Na-activated bentonite therefore supports its suitability for such applications.

In contrast, dehydroxylation and the collapse of the montmorillonite structure following heating to 800 °C (Figs. 2, 3, and 6) resulted in a complete loss of swelling capacity (Fig. 7).

Tab. 5. Volume of the initial dry bentonites and their swell indices before and after drying and heating. All values are given in ml.

Temperature	RLU	ELU
25 °C dry	2	2
25 °C	24.5	5
105 °C	26	6
200 °C	25	6.5
400 °C	10	2.25
800 °C	2	2

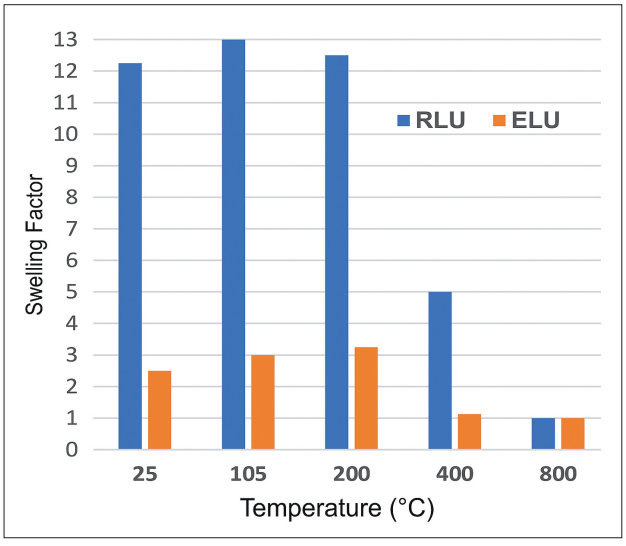

Fig. 7. Swelling factor calculated from swell index of bentonites before and after thermal treatment.

4. CONCLUSIONS

Bentonites represent an important mineral resource for the Slovak economy due to their extensive extraction and export, as well as their considerable potential in addressing current societal and technological challenges, particularly deep geological disposal of radioactive waste and the decarbonization of the construction sector. This study provides the first comprehensive data on the hydration, dehydration, rehydration, and dehydroxylation behaviour of bentonites from the Lutila I deposit. The obtained results contribute to a better understanding of the thermal and hydration-related transformations of these materials and provide essential information for evaluating their suitability for a wide range of applications, including those associated with radioactive waste management and supplementary cementitious materials.

In this study, two commercial bentonite samples from the Lutila I deposit (one of the most promising bentonite resources in Slovakia) were investigated. The Na-activated sample (RLU) contained 55 wt.% montmorillonite, whereas the non-activated sample (ELU) contained 67 wt.% montmorillonite. The dehydration behaviour of both bentonite samples was characterized by the presence of weakly bound water released at approximately 105 °C and strongly bound water released up to 250 °C. The markedly higher LOD value of the ELU sample was only partly related to its greater montmorillonite abundance and was predominantly controlled by the nature of the exchangeable cations. Specifically, hydrated divalent Ca^{2+} and Mg^{2+} cations in the ELU bentonite promoted the retention of two interlayer water layers, whereas hydrated monovalent Na^{+} cations in the RLU bentonite were associated with a single interlayer water layer.

Both studied bentonites contained two hydrated phases, montmorillonite (55.5 and 67 wt.%) and Opal-C/CT (25 and 9 wt.%), which are difficult to separate; consequently, the allocation of the determined mass loss to these individual phases is complicated. Nevertheless, an attempt was made to distinguish the respective contributions on the basis of the data obtained in this study, supplemented by previously published findings. The mass loss observed up to 200 °C was attributed predominantly to molecular water associated with montmorillonite. Weakly bound molecular water was released from the interlayer space of montmorillonite to 105 °C, whereas the gradual release of more strongly bound water continued up to 200 °C and, to a lesser extent, at higher temperatures. During the thermal treatment of the two Lutila I bentonite samples within the temperature range of 200–800 °C, three principal processes were identified. First, the gradual release of tightly bound interlayer water from montmorillonite occurred up to approximately 250 °C. Second, the dehydroxylation of montmorillonite commenced between 500 and 550 °C, reaching a maximum at approximately 665 °C with gradual termination up to 800 °C. Third, the release of water associated with Opal-C/CT began at approximately 350 °C and proceeded predominantly up to 600 °C, in agreement with the observations of Thomas et al. (2020). Based on the TGA mass loss between 200 and 800 °C, the phase abundances obtained by QXRD, and the published dehydroxylation mass loss of pure montmorillonite, the contributions of montmorillonite and opal-C/CT to the total water loss were estimated. For sample RLU, the respective contributions were calculated to be 2.64 and 3.12 wt.%, whereas corresponding values of 3.22 and 0.64 wt.% were obtained for sample ELU.

The thermal behaviour of the investigated bentonites suggested that the nature of the exchangeable cations could play an important role in determining their suitability as supplementary cementitious materials, along with more frequently considered factors such as calcination temperature and time, and mineral composition. Heating the ELU sample with Ca^{2+} and Mg^{2+} as exchangeable cations to 800 °C resulted in the crystallization of a new phase, $MgAl_2Si_4O_{12}$ with a high-quartz structure, reducing the content of the amorphous component responsible for pozzolanic reactivity. In contrast, the Na-activated RLU sample underwent structural collapse without the formation of secondary crystalline phases, promoting the development of an amorphous phase and thus exhibiting a higher potential for SCM utilization.

The results also highlighted the potential of domestic Na-activated bentonite (RLU) for application in deep geological disposal of radioactive waste, as demonstrated by its substantially higher swelling capacity compared with the non-activated bentonite. In addition, the partial preservation of rehydration and swelling capacity following heating to 400 °C suggests that key barrier functions may be retained under thermally stressed conditions.

Acknowledgements: The work was supported by the projects APVV-24-0643 and UK/3062/2024 (Funded by the EU NextGenerationEU through the Recovery and Resilience Plan for Slovakia under the project No. 09I03-03-V05-00012). We would like to thank to REGOS, s.r.o. and Envigeo, a.s. for providing samples. We thank P. Bačík and his team for measuring XRD patterns.

References

Adamcová R., Suraba V., Krajňák A., Rosskopfová O. & Galamboš M., 2014: First shrinkage parameters of Slovak bentonites considered for engineered barriers in the deep geological repository of high-level radioactive waste and spent nuclear fuel. *Journal of Radioanalytical and Nuclear Chemistry*, 302, 1, 737–743.

Andrejkovičová S., Rocha F., Janotka I. & Komadel P., 2008: An investigation into the use of blends of two bentonites for geosynthetic clay liners. *Geotextiles and Geomembranes*, 26,436–445.

ASTM D5890, 2011, Standard Test Method for Swell Index of Clay Mineral Component of Geosynthetic Clay Liner, ASTM International, West Conshohocken, PA, www.astm.org

Avet F., Snellings R., Alujas Diaz A., Ben Haha M. & Scrivener K., 2016: Development of a new rapid, relevant and reliable (R3) test method to evaluate the pozzolanic reactivity of calcined kaolinitic clays. *Cement and Concrete Research*, 85, 1–11.

Ayati B., Newport D., Wong H. & Cheeseman C., 2022: Low-carbon cements: Potential for low-grade calcined clays to form supplementary cementitious materials. *Cleaner Materials*, 5, 100099.

Badogiannis E. & Tsivilis S., 2009: Exploitation of poor Greek kaolins: Durability of metakaolin concrete. *Cement and Concrete Composites*, 31, 2, 128–133.

Bahranowski K., Klimek A., Gaweł A. & Serwicka E.M., 2021: Rehydration driven Na-activation of bentonite–evolution of the clay structure and composition. Materials, 14, 7622.

Baláž P., Stupák J., Radvanec M., Mikušová J., Fajtová D., Nováčková M., Španek P., Šesták P., Frajkor V. & Mihaľ I., 2015: Surovinový potenciál Slovenskej republiky – analýza vybraných nerastných surovín, regionálny geologický výskum, Číslo geologickej úlohy: 607 12. Záverečná správa. [Raw material potential of the Slovak Republic – analysis of selected mineral resources, regional geological research, Geological task number: 607 12. Final report]. Bratislava, Geofond. State Geological Institute of Dionyz Stur, Geofond, Archive number: 95139, Bratislava, 157 p. [in Slovak]

Bačuvčík M., Mendel J. & Janotka I., 2022: Non-Expandable Perlite Powder as Pozzolanic Addition in Concrete. *ACI Materials Journal*, 119, 4, 3–14.

Bizovská V., Pálková H. & Madejová J., 2016: Near-infrared study of water adsorption on homo-ionic forms of montmorillonite. *Clays and Clay Minerals,* 64, 571–585.

Carrado K. A. & Komadel P., 2009: Acid activation of bentonites and polymer-clay nanocomposites. *Elements*, 5, 2, 111–116.

Christidis G. (Ed.), 2011: Advances in the characterization of industrial minerals. EMU Notes in Mineralogy, 9, The Mineralogical Society of Great Britain and Ireland, 485 p.

Christidis G.E., 2013: Assessment of Industrial Clays. *In*: Bergaya F., Lagaly G. (Eds.): Handbook of Clay Science, Developments in Clay Science, 5, the 2nd edition. Elsevier, pp. 425–449.

Christidis G.E. & Huff W.D. 2009: Geological aspects and genesis of bentonites. *Elements* 5, 2, 93–98.

Coutelle H., Deher A., Kaufhold S., Karidakis T., Kesore K., Koch D., Krause A., Rikertsen N. & Stützer A., 2024a: Aplications. *In*: Kaufhold S. (Ed.): Bentonites: Characterization, Geology, Mineralogy, Analysis, Mining, Processing and Uses. Bundesanstalt Für Geowissenschaften und Rohstoffe (BGR), pp. 221–274.

Coutelle H., Kesore K., Koch D. A., Kaufhold S., Rikertsen N. & Stützer A., 2024b: Processing. *In*: Kaufhold S. (Ed.): Bentonites: Characterization, Geology, Mineralogy, Analysis, Mining, Processing and Uses. Bundesanstalt Für Geowissenschaften und Rohstoffe (BGR), pp. 199–220.

Čičel B., Komadel P., Bednáriková E. & Madejová J. 1992: Mineralogical composition and distribution of Si, AI, Fe, Mg and Ca in the fine fractions of some Czech and Slovak bentonites. *Geologica Carpathica, Ser. Clays*, 1, 1, 3–7.

Derkowski A., Drits V. A. & McCarty D. K., 2012: Rehydration of dehydrated-dehydroxylated smectite in a low water vapor environment. *American Mineralogist*, 97, 110–127.

Derkowski A. & Kuligiewicz A., 2022: Thermal analysis and thermal reactions of smectites: a review of methodology, mechanisms, and kinetics. *Clays and Clay Minerals*, 70, 946–972.

Drits V., Besson G. & Muller F., 1995: An improved model for structural transformation of heat-treated aluminous dioctahedral 2:1 layer silicates. *Clays and Clay Minerals*, 43, 718–731.

Eberl D. D., 2003: User's guide to RockJock – A program for determining quantitative mineralogy from powder X-ray diff raction data. U.S. Geological Survey, Open–File Report, 78, 47 p.

Eisenhour D. & Brown R., 2009: Bentonite and Its Impact on Modern Life. *Elements*, 5, 2, 83–88.

Emmerich K.: 2010 Thermal analysis in the characterization and processing of industrial minerals. *In* Christidis, G. E. (Ed.): Advances in the Characterization of Industrial Minerals. European Mineralogical Union, pp. 129–170.

Emmerich, K., 2013: Full Characterization of Smectites. *In*: Bergaya, F., Lagaly, G. (Eds.): Handbook of Clay Science, Developments in Clay Science, 5B, the 2nd edition. Elsevier, pp. 381–404.

Emmerich K., Giaudo N., Schuhmann R., Schnetzer F., Kaden H. & Thissen P., 2018: On the prediction of water contents in Na-saturated dioctahedral smectites. *Journal of Physical Chemistry C*, 122(13), 7484–7493.

Emmerich K., Wolters F., Kahr G. & Lagaly G., 2009: Clay profiling: the classification of montmorillonites. *Clays and Clay Minerals*, 57, 104–114.

Fajnor V. Š. & Kuchta Ľ, 1985: Effect of magnesium and calcium on the high-temperature reactions of synthetic montmorillonite. *Thermochimica Acta*, 93, 549–552.

Fernandez R., Martirena F. & Scrivener K. L., 2011. The origin of the pozzolanic activity of calcined clay minerals: a comparison between kaolinite, illite and montmorillonite. *Cement and Concrete Research,* 41, 113–122.

Ferrage E., 2016: Investigation of the interlayer organization of water and ions in smectite from the combined use of diffraction experiments and molecular simulations. A review of methodology, applications, and perspectives. *Clays and Clay Minerals*, 64, 348–373.

Flörke O. W., Graetsch H., Martin B., Röller K. & Wirth R., 1991: Nomenclature of micro and non-crystalline silica minerals, based on structure and microstructre. *Neues Jahrbuch Mineralogie und Petrologie, Abhandlungen*, 163, 19–42.

Galamboš M., Kufčáková J. & Rajec P., 2009: Sorption of strontium on Slovak bentonites. *Journal of Radioanalytical and Nuclear Chemistry*, 281, 347–357.

Garg N. & Skibsted J., 2014: Thermal activation of a pure montmorillonite clay and its reactivity in cementitious systems. *The Journal of Physical Chemistry C*, 118, 11464–11477.

Gilg H. A., Kaufhold S. & Ufer K., 2024: Smectite and bentonite terminology, classification, and genesis. *In:* Kaufhold S. (Ed.): Bentonites: Characterization, Geology, Mineralogy, Analysis, Mining, Processing and Uses. Bundesanstalt Für Geowissenschaften und Rohstoffe (BGR), pp. 15–32.

Górniak K., Szydlak T., Gawel A., Klimek A., Tomczyk A., Sulikowski B., Olejniczak Z., Motyka J., Serwicka E. M. & Bahranowski K. 2016: Commercial bentonite from the Kopernica deposit (Tertiary, Slovakia): a petrographic and mineralogical approach. *Clay Minerals*, 51, 97–122.

Graetsch H., 1994. Structural characteristics of opaline and microcrystalline silica minerals. *In*: Heaney, P.J., Prewitt, C.T., Gibbs, G.V. (Eds.): Silica. Physical Behavior, Geochemistry and Materials Applications. Reviews in Mineralogy, 29. Mineralogical Society of America, pp. 209–232.

Gread F. A., Kureková V., Santamaría-López Á., Osacký M. & Uhlík P., 2025: Near-infrared as a swift method to quantify dioctahedral smectite content in bentonite. *Applied Clay Science*, 269, 1–14.

Gread F. A., Osacký M., Kureková V., Pálková H., Hudec P., Brčeková J., Milovský R., Mihaľ M., Biroň A., Šurka J. & Uhlík P., 2026: Characterization of Michaľany – Lastovce Bentonite-Like Deposit, East Slovakia. *Clays and Clay Minerals*, accepted.

Gregor M. & Čičel B., 1969: Bentonit a jeho využitie. [Bentonite, a new basic material of the industry]. SAV, Bratislava, 401 p. [in Slovak]

Grim R. E., 1962: Applied Clay Mineralogy. Me Graw-Hill, Book Company. Inc., New York, Toronto, London, 316–330.

Grim R. E. & Güven N., 1978: Bentonites: geology, mineralogy, properties, and uses. Developments in Sedimentology, 24. Elsevier, 256 p.

Grim R. E. & Kulbicki G. 1961: Montmorillonite: high temperature reactions and classification. *American Mineralogist*, 46, 1329–1369.

Hlavný banský úrad, 2025: Správa o činnosti Hlavného banského úradu a obvodných banských úradov SR za rok 2024. [Report on the activities of the Main Mining Office and District Mining Offices of the Slovak Republic for 2024] Banská Štiavnica, 133 p. [in Slovak]

Honty M., Uhlík P., Šucha V., Čaplovičová M., Franců J., Clauer N., & Biroň A., 2004: Smectite-to-illite alteration in salt-bearing bentonites (The East Slovak Basin). *Clays and Clay Minerals*, 52, 533–551.

Hotton C., Bizien T., Hamon C., Ferrage, E. & Paineau E., 2025: Bridging the gap between osmotic and crystalline swelling in 2d layered materials using levitated droplets. *Small*, 21, 2505038.

Janotka I., Kiss S. & Baslik R., 2002: Geosynthetic mat Tatrabent - development, production and application. *Applied Clay Science*, 21, 21–31.

Janotka I., Puertas F., Palacios M., Kuliffayová M. & Varga C., 2010: Metakaolin sand–blended-cement pastes: Rheology, hydration process and mechanical properties. *Construction and Building Materials*, 24, 791–802.

Jones B., 2021: Siliceous sinters in thermal spring systems: Review of their mineralogy, diagenesis, and fabrics. *Sedimentary Geology*, 413, 105820.

Kaufhold S., Dohrmann R. & Ufer K., 2016: Interaction of Magnesium Cations with Dioctahedral Smectites under HLRW Repository Conditions. *Clays and Clay Minerals*, 64, 743–752.

Kaufhold S., Dohrmann R., Wallis I., & Weber C., 2023: Chemical and mineralogical reactions of bentonites in geotechnical barriers at elevated temperatures: review of experimental evidence and modelling progress. *Clay Minerals*, 58(3), 280–300.

Komadel P. & Madejová J., 2013: Acid activation of clay minerals. *In*: Bergaya F., Lagaly G. (Eds.): Handbook of Clay Science, Developments in Clay Science, 5A, the 2nd edition. Elsevier, pp. 386–409.

Kraus I., Čičel B. & Machajdik D., 1982: Origin and genesis of the clays resulting from alteration of rhyolite volcanic rocks in Central Slovakia. *Geologica Carpathica*, 33, 269–275.

Kraus I., Hroncová Z., Horský S. & Mihalič A., 1989: Ložiská a výskyty bentonitov SSR. [Deposits and occurrences of bentonite in the Slovak Socialist Republic] *Mineralia Slovaca*, 21, 525–531. [in Slovak with English summary]

Kraus I., Šamajová E., Šucha V., Lexa J. & Hroncová Z., 1994: Diagenetic and hydrothermal alterations of volcanic rocks into clay minerals and zeolites (Kremnické Vrchy Mts., the Western Carpathians). *Geologica Carpathica*, 45, 3, 151–158.

Kuligiewicz A. & Derkowski A., 2017: Tightly bound water in smectites. *American Mineralogist*, 102, 1073–1090.

Lang L. Z., Xiang W., Huang W., Cui D. S., Schanz T., 2017: An experimental study on oven-drying methods for laboratory determination of water content of a calcium-rich bentonite. *Applied Clay Science*, 150, 153–162.

Lexa J., Halouzka R., Havrila M., Hanzel V., Kubeš P., Liščák P. & Hojstričová V., 1998: Explanatory notes to the geological map of Kremnické vrchy mountain range. Geological Survey of Slovak Republic, Bratislava, 308 p. [in Slovak with English summary]

Madejová J., Gates W. P. & Petit, S., 2017: IR spectra of clay minerals. *In:* Gates W. P., Kloprogge J. T., Madejová J., & Bergaya F. (Eds.): Infrared and Raman spectroscopies of clay minerals, Developments in Clay Science, 8, pp. 107–149.

Madejová J., Kraus I. & Komadel P., 1995: Fourier transform infrared spectroscopic characterization of dioctahedral smectites and illites from the main Slovak deposits. *Geologica Carphatica - Clays*, 4, 23–32.

Min Y., Kabir H., Kothari C., Igbal M.F. & Garg N., 2025: UR^2: Ultra-rapid reactivity test for real-time, low-cost quality control of calcined clays. *Cement and Concrete Research*, 191, 107806.

Moore D. M. & Reynolds Jr, R. C., 1997: X-ray diffraction and the identification and analysis of clay minerals. 2nd ed. Oxford University Press, New York, 378 p.

Murray H. H., 2007: Applied Clay Mineralogy - Occurrences, Processing and Applications of Kaolins, Bentonites, Palygorskite-Sepiolite, and Common Clays. Developments in Clay Science, 2. Elsevier, 180 p.

Omotoso O. & Eberl D. D., 2009: Sample preparation and data collection strategies for X-ray diffraction quantitative phase analysis of clay-bearing rocks. *In:* 46th Annual Meeting of the Clay Minerals Society. Billings, Montana, 1–209.

Osacký M., Binčík T., Paľo T., Uhlík P., Madejová J. & Czimerová A., 2019: Mineralogical and physico–chemical properties of bentonites from the Jastrabá Formation (Kremnické vrchy Mts., Western Carpathians). *Geologica Carpathica*, 70, 5, 433–445.

Pentrák M., Hronský V., Pálková H., Uhlík P., Komadel P. & Madejová J. 2018: Alteration of fine fraction of bentonite from Kopernica (Slovakia) under acid treatment: a combined XRD, FTIR, MAS NMR and AES study. *Applied Clay Science*, 163, 204–213.

Rybka K., Kuligiewicz A., Kaufhold S., Dohrmann R. & Derkowski A., 2025: Kinetics of rehydration in smectite and its application to water resorption in bentonites. *Applied Clay Science*, 271, 107813.

Salles F., Bildstein O., Douillard J. M., Jullien M., Raynal J. & Van Damme H., 2010: On the cation dependence of interlamellar and interparticular water and swelling in smectite clays. *Langmuir*, 26, 7, 5028–5037.

Salles F., Douillard J. M., Bildstein O., El Ghazi S., Prélot B., Zajac J., & Van Damme H., 2015: Diffusion of interlayer cations in swelling clays as a function of water content: Case of montmorillonites saturated with alkali cations. *The Journal of Physical Chemistry* C, 119, 19, 10370–10378.

Sellin P. & Leupin O. X., 2013: The use of clay as an engineered barrier in radioactive waste management – a review. *Clays and Clay Minerals*, 61, 477–498.

Schulz H. Muchow G. M., Hoffmann W. & Bayer G., 1971: X-ray study of Mg-Al silicate high-quartz phases. *Zeitschrift für Kristallographie*, 133, 91–109.

Schulze S. E. & Rickert J., 2019: Suitability of natural calcined clays as supplementary cementitious material. *Cement and Concrete Composites*, 95, 92–97.

Shannon R. D., 1976: Revised effective ionic radii and systematic studies of interatomic distances in halides and chalcogenides. *Acta Crystallographica A*, 32, 751–767.

Simmons K. J., 2025: Clays. *In:* U.S. Geological Survey, Mineral Commodity Summaries 2025 (ver. 1.2, March 2025), 60–61 pp.

Slaný M., Kuzielová E., Žemlička M., Matejdes M., Struhárová A. & Palou M. T., 2023: Metabentonite and metakaolin-based geopolymers/zeolites: relation between kind of clay, calcination temperature and concentration of alkaline activator. *Journal of Thermal Analysis and Calorimetry*, 148, 20, 10531–10547.

Slávik J., Hruškovič, S., Očenáš, D. & Zuberec, J., 1971: Ložiská bentonitov na Slovensku. [Deposits of Bentonites in Slovakia] *Mineralia Slovaca*, 3, 12–13, 561–573. [in Slovak]

Smith D. W., 1977: Ionic hydration enthalpies. *Journal of Chemical Education*, 54, 9, 540–542.

Snellings R. & Scrivener K. L., 2016: Rapid screening tests for supplementary cementitious materials: past and future. *Materials and Structures*, 49, 3265–3279.

Snellings R., Suraneni P. & Skibsted J., 2023: Future and emerging supplementary cementitious materials. *Cement and Concrete Research*, 171, 107199.

Steudel A., Batenburg L., Fischer H., Weidler P. G. & Emmerich K, 2007: Alteration of swelling clay minerals by acid activation. *Applied Clay Science*, 44, 105–115.

Šoltés S., Kúšik D., Mižák J. & Kubač A., 2024. Slovak Minerals Yearbook 2023, State Geological Institute of Dionyz Stur, Bratislava, 73–76 p.

Środoń J., Drits V. A., McCarty D. K., Hsieh J. C. C. & Eberl D. D., 2001: Quantitative X-ray diffraction analysis of clay-bearing rocks from random preparations. *Clays and Clay Minerals*, 49, 514–528.

Środoń J., & McCarty D. K., 2008: Surface area and layer charge of smectite from CEC and EGME/H2O-retention measurements. *Clays and Clay Minerals*, 56, 155–174.

Šucha V., Adamcová R., Bujdák J., Haasová Z., Honty M., Komadel P., Kufčáková J., Madejová J., Rajec P., Stríček I., Uhlík P. & Valúchová J., 2005: Fyzikálne a mechanické vlastnosti tesniacich materiálov pre úložisko RAO. [Physical and

mechanical properties of sealing materials for radioactive waste storage]. ZS Štátneho programu výskumu a vývoja: Výskum vlastností a využitia vybranej skupiny nerastných surovín, Katedra ložiskovej geológie, Prírodovedecká fakulta, Univerzita Komenského v Bratislave, Bratislava, 281 p. [in Slovak]

Theng B.K.G. (Ed.), 2012: Formation and Properties of Clay-Polymer Complexes. Developments in Clay Science, 4, Elsevier, 511 p.

Thomas P., Chauviré B., Flower-Donaldson K., Aldridge L., Smallwood A. & Liu B., 2020: FT-NIR and DSC characterisation of water in opal. *Ceramics International*, 46, 18, Part B, 29443–29450.

Trümer A., Ludwig H.-M., Schellhorn M. & Diedel R., 2019: Effect of a calcined Westerwald bentonite as supplementary cementitious material on the long-term performance of concrete. *Applied Clay Science*, 168, 36-42.

Tsipursky S. I. & Drits V. A., 1984: The distribution of octahedral cations in the 2:1 layers of dioctahedral smectites studied by oblique texture electron diffraction. *Clay Minerals*, 19, 177–192.

Uhlík P., Jánošík M., Kraus I., Pentrák M. & Čaplovičová M. 2012: Characterisation of bentonite from Hliník nad Hronom deposit (Jastrabá Formation of the Štiavnica stratovolcano, Western Carpathians). *Acta Geologica Slovaca* 4, 125–137. [in Slovak with English summary]

Uhlík P., Lexa J., Biroň A., Mohamed Gread F., Brčeková J., Osacký M. & Koděra P., 2024. Slovak bentonite deposits – a brief overview. *In:* 61st Annual Meeting of The Clay Minerals Society and 5th Asian Clay Conference. Honolulu: The Clay Mineral Society (CMS), 2024, pp. 289–289.

Varga P., Uhlík P., Lexa J., Šurka J., Bizovská V., Hudec P. & Pálková H. 2019: The influence of porosity on the release of water from perlite glass by thermal treatment. *Monatshefte für Chemie,* 150, 1025–1040.

Webb S. W., Stanley D. A. & Scheiner B. J., 1986: Thermal analysis of ion-exchanged montmorillonite. *Particulate Science and Technology*, 4, 2, 131–142.

Wolters F. & Emmerich K., 2007: Thermal reactions of smectites—Relation of dehydroxylation temperature to octahedral structure. *Thermochimica Acta*, 462, 1–2, 80–88.

Zuberec J., Tréger M., Lexa J. & Baláž P., 2005: Mineral resources of Slovakia. Štátny geologický ústav Dionýza Štúra, Bratislava, 350 p.